

Hybrid desalination system of mechanical vapor recompression based on membrane distillation

Yinan Wang¹, Boya Qiu¹, Zeyi Xiao^{*1}, Jingyun Liu¹, Senqing Fan¹ and Xiaoyu Tang²

¹School of Chemical Engineering, Sichuan University, No.24 South Section 1, Yihuan Road, Chengdu, China

²Biogas Institute of Ministry of Agriculture, Section 4-13, Renmin Nan Road, Chengdu, China

(Received October 20, 2020, Revised May 3, 2021, Accepted May 12, 2021)

Abstract. The microporous PTFE membrane was used for membrane distillation (MD) experiment and presented ultra-high efficiency of desalination. A hybrid desalination system combining membrane distillation and mechanical vapor compression (MD+MVR) had been developed on the basis of the MD experiment. The system featured that the latent heat and part of sensible heat of vapor from the MVR were recovered to heat the MD process, and the heating process occurred in the same module as the MD process. Models were built according to the energy and mass conservation for the system description. Based on the simulation and experimental data, when the system was assigned a treatment capacity 1000 kg h⁻¹ for 1% saline water and with corresponding 875 kg h⁻¹ fresh water production, it would be stuffed with 75.24 m² of PTFE membrane and expense only 3.31 kW of electrical power, under 353 K of feed temperature in membrane module and 26 kPa of compressor suction pressure. The compressor power requirement would trade off the heat transfer area with variation of the heat transfer temperature difference. The higher the salinity concentration in the residual concentrate after distillation was, the higher the compressor power, membrane area and heat exchanger area would be.

Keywords: membrane distillation; bi-axial stretching PTFE membrane; desalination; mechanical vapor recompression; process thermodynamics

1. Introduction

Water utilization are facing severe challenges due to the shortage of freshwater resources and the deterioration of the ecological environment. With the serious of global water pollution, desalination technologies have received widespread attention in recent years, especially in the process of high salinity wastewater treatment with the mass concentration more than 1%, such as shale gas fracturing flowback fluid. (Chang *et al.* 2019, Gao *et al.* 2018, Ihsanullah *et al.* 2021). There are various desalination patterns based upon conventional evaporation process, mainly including single effect evaporation (SEE), multiple effect evaporation (MEE), multi-stage flash (MSF), thermal vapor compression (TVC) and mechanical vapor recompression (MVR) at present (Kariman *et al.* 2019, Lv *et al.* 2019, Onishi *et al.* 2017, Zhou *et al.* 2019).

In recent decades, innovative membrane technologies have been developed for desalination of saline water and sea water to produce fresh water or treat wastewater, such as nanofiltration (NF), reverse osmosis (RO) and membrane distillation (MD) (El-ghzizel *et al.* 2019, Hilal *et al.* 2015, Luo *et al.* 2017). In both RO process and NF process, the water stream through membranes has no phase change from liquid to vapor, and they can achieve higher flux rather than desalination efficiency and fresh water recovery. Different

from the RO and NF, MD is a heat-driven interfacial evaporation process. In MD process, the hydrophobic microporous membranes provide enormous microporous interfacial area and impede liquid flow-through owing to the hydrophobicity of membranes, which can ensure most perfect desalination efficiency and acceptable flux. The driving force for mass transfer is the difference of vapor pressure between the liquid and the vapor side of the membranes (Wang *et al.* 2016). MD has become one of the most attractive desalination systems, owing to its advantages of high purity of product, the reduced vapor space and having the possibility of operating at lower temperatures (Boutikos *et al.* 2017). Moreover, it is low sensitive to concentration polarization and fouling, as well as capable to use low-temperature waste heat and renewable energy sources, such as solar and geothermal energy (Ahmed *et al.* 2020, Luo and Lior 2017). During MD desalination, the permeate flux is directly proportional to the vapor pressure difference between the two sides of the membrane (Kim *et al.* 2018). In order to increase the system energy efficiency, multi-effect MD should be developed. It has been reported that higher feed temperature could also improve MD system thermal efficiency, since heat transfer is enhanced (Boutikos *et al.* 2017).

As one of the advanced evaporative technologies, the vapor produced from the evaporator during the MVR process can be reused to heat solution with higher efficiency than SEE, MSF, MEE and TVC (Alasfour and Abdulrahim 2011). Currently, most of the reported on the MVR are focused on description of system design and operation performance (Dahmardeh *et al.* 2019, Liang *et al.*

*Corresponding author, Professor
E-mail: mgch@scu.edu.cn

2017). For example, the energy consumption is in the range of 10 to 13 kW h m⁻³ for a single-effect MVR desalination system, according to second law of the thermodynamics and thermo economic analysis (Jamil and Zubair 2017). Compared with single-effect MVR, the power consumption of the double-effect MVR system is lower. The power consumption of the double-effect MVR system can be increased with evaporation temperature decreases and the minimum power consumption can be achieved when the first effect emission concentration is approximately 32 wt% (Liang *et al.* 2013). The combination of MVR and other energy producing technologies is great important, especially in the areas of electric power shortage or enriched with renewable energy. For example, a wind driven MVR system with turbine diameters of 43 m has been developed to apply in windy area of Red Sea with the average wind speed of 7 m s⁻¹ for the production of fresh water. In the hybrid system, 938 m³ of fresh water could be produced per day, which is adequate for communities around 2350 unit (Karameldin *et al.* 2003). MVR is also well suited for integration with other energy-dependent technologies. For example, a system combining MD and MVR has been proposed to treat sulfuric acid waste treatment theoretically based on the MD experiment with pure water (Si *et al.* 2019, 2020).

Energy efficiency and compact volume are two important issues for a desalination system. Greater evaporation area can be achieved in MD, under the same space with porous membrane. Moreover, the membrane used in MD has the advantages of nice adaptability to high salinity wastewater and replaceable, compared with traditional evaporator with metal material. However, the thermal efficiency is low and it needs a constantly heat source to provide the mass transfer driven force. MD is hardly accomplished on a large scale. MVR is an energy efficient evaporation technology. However, a compact volume can be hardly realized for MVR, since the structure of evaporator is complicated. Furthermore, it easily suffers from corrosion and scaling during the operation. Combing of MD and MVR can make full use of their advantages. Therefore, high energy efficiency and compact volume can be achieved in this hybrid system. The aims of this study are to design a hybrid system combined MD and MVR for desalination and develop a mathematical model to explore the operation performance of the system. This is the report to simulate the desalination performance of a combined MD and MVR system based on MD experiment for desalination with bi-axial stretching microporous PTFE membrane.

2. Desalination experiment of MD

Experiments of desalination by membrane distillation were conducted. The bi-axial stretching microporous polytetrafluoroethylene (PTFE) membranes with average pore size 0.6 microns, porosity 0.7 and thickness 60 microns, were applied to the experimental MD process. PTFE membranes had much perfect features, such as outstanding thermal and chemical stability. Due to its ultra-high hydrophobicity, PTFE would be promising

Table 1 The operating parameters of membrane distillation

Parameters	Value
Absolute pressure in vapor side, kPa	9
Flowrate of feed, kg h ⁻¹	120
Area of membrane, m ²	0.024
Mass transfer coefficient of membrane, s m ⁻¹	1.13
Concentration of feed, %	1, 4, 8
Temperature, K	303~333

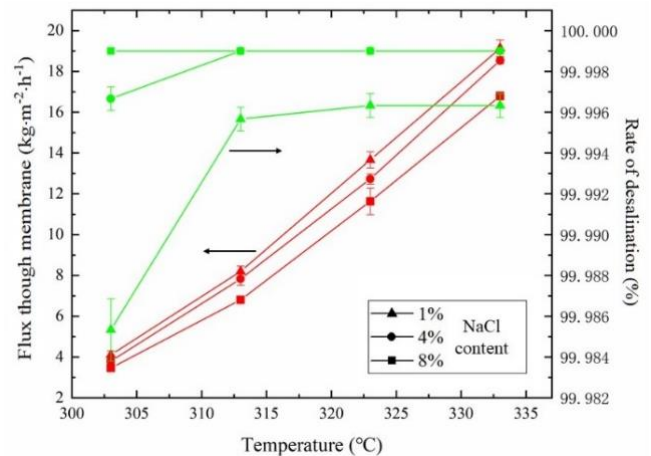


Fig. 1 The effect of temperature changes on the flux through membrane and desalination efficiency in MD

membrane material for MD process. The conductivity of some certain concentrations of NaCl solution prepared using ultrapure water (conductivity of 0) was measured and a concentration-conductivity standard curve was plotted. A series of MD experiments with different NaCl concentrations at different temperatures were done. The mass and conductivity of the vapor condensate were tested to derive the permeate flux and desalination efficiency. The mass transfer coefficient of membrane was fitted through the relationship between permeate flux and vapor pressure difference. The operation and performance data were summarized in Table 1 and Fig. 1, respectively, which were taken as fundamental data of process design.

As could be seen in Fig. 1, the flux through membrane was greatly depended upon the temperature in MD rather than the feed concentration. It might be due to the change in the vapor pressure of brine. When the absolute pressure (vacuum degree) of vapor side in the membrane module was constant, higher temperature would produce higher vapor pressure of liquid side, and then result in higher driving force for MD. Consequently, the temperature and heat exchange in the membrane module would be main effects on MD performance and the system.

Overall, PTFE membranes exhibited excellent desalination performance at various concentrations and temperatures from Fig. 1. When the brine concentration was 1% and the temperature was 303 K, the rate of desalination was 99.985%, and when the temperature was more than 313 K, the rate of desalination was 99.999% for both 4% and 8% of the brine concentration.

and the concentrated solution. The input mass of the system should be equal to the output mass of the system, which could be described as follows:

$$M_1 = M_9 + M_{12} \quad (1)$$

$$X_1 M_1 = X_{12} M_{12} \quad (2)$$

where, M is the mass flow rate; X is the mass concentration.

The input energy of the system included the enthalpy of the feed and the compression work against the vapor by the vapor compressor. The output energy of the system included the enthalpy of condensate water and the concentrated solution. Therefore, the energy balance for the system could be described as follows:

$$X_1 M_1 + P_i = H_9 M_9 + H_{12} M_{12} \quad (3)$$

where H is the specific enthalpy; P_i is the ideal power required by vapor compressor.

4.2 Heat transfer in preheaters

Two plate heat exchangers were introduced as the preheaters. The cold feed would be heated by the condensate water and the concentrated solution through the preheaters. The heat absorbed by the feed could be equal to that released from the condensate water and the concentrated solution, which could be described as follows:

$$Q_1 = M_8 C_{p8} T_8 - M_9 C_{p9} T_9 = M_3 C_{p3} T_3 - M_2 C_{p2} T_2 \quad (4)$$

$$\begin{aligned} Q_2 &= M_{10} C_{p10} T_{10} - M_{12} C_{p12} T_{12} \\ &= M_3' C_{p3} T_3' - M_2' C_{p2} T_2' \end{aligned} \quad (5)$$

where, C_p is the specific heat at constant pressure; T is the temperature.

4.3 Mass and heat transfer in membrane module

The input mass of the membrane module included the feed and the compressed vapor. The output mass of the membrane module included the permeate vapor, the retentate and the condensate water. The input mass and output mass of the membrane module should be equal according to the mass conservation, which could be described as follows:

$$M_4 + M_7 = M_5 + M_6 + M_8 \quad (6)$$

In general, the membrane flux during MD was directly proportional to the pressure difference of vapor between the two sides of the membrane, which could be described as follows (Kim *et al.* 2018):

$$F = K_m (P_v - P_p) \quad (7)$$

where, F is the membrane flux during MD; K_m is the mass transfer coefficient characterized by the membrane performance during MD, which is a constant number and here calculated as 1.13 s m^{-1} according to the MD experiment for the biaxial stretch polytetrafluoroethylene

membrane; P_p is the pressure of the permeate vapor on the vapor side of the membrane and is equal to the compressor suction pressure P_c ; P_v is the saturated vapor pressure of the feed on the liquid side of the membrane, which could be described as follows:

$$P_v = \gamma_w x_w P_w \quad (8)$$

where, γ_w and x_w are the activity coefficient and molar fraction of water at the liquid-vapor interface, respectively. The activity coefficient denotes the deviations from ideal behavior in a mixture of chemical substances. For an aqueous solution with NaCl, the activity coefficient is described as follows:

$$\gamma_w = 1 - 0.5x_s - 10x_s^2 \quad (9)$$

where, x_s is the molar fraction of NaCl in saline solution.

P_w in Eq. (8) is the saturation pressure of pure water (in P_a), which is determined by using the Antoine equation as follows:

$$\ln P_w = \left(23.238 - \frac{3841}{T_{fm} - 45} \right) \quad (10)$$

where, T_{fm} is the temperature of fluid on the membrane surface.

The evaporation capacity of the membrane system could be calculated by multiplying the flux and effective area of the membrane, described as follows:

$$M_6 = A_m F \quad (11)$$

where, A_m is the effective area of the membrane.

The heat transfer from the compressed vapor to the feed in the membrane module was related to the coefficient, area and temperature difference of heat transfer, described as follows:

$$Q = UA \cdot \Delta T \cdot CF \quad (12)$$

where, Q is heat flow rate; U is the total coefficient of heat transfer between the condensate and solution; A is area of heat transfer; ΔT is the heat transfer temperature difference between the compressed vapor and feed; CF is the correction coefficient for plate combination.

The total coefficient of heat transfer was mainly composed of the coefficient convective heat transfer between the feed and the plate, the conductivity of the plate and the coefficient of condensation heat transfer, which could be described as follows:

$$\frac{1}{U} = \frac{1}{h_c} + \frac{1}{h_{con}} + \frac{\delta}{k} \quad (13)$$

where, h_c is the coefficient of convective heat transfer; h_{con} is the coefficient of condensation heat transfer; δ is the thickness of the plate, k is the conductivity of the plate.

The coefficient of convective heat transfer between the feed and the plate could be described as follows:

$$h_c = 0.336 \frac{k}{d} \left(\frac{d\rho u}{\mu} \right)^{0.634} \left(\frac{c_p \mu}{k} \right)^{0.4} \quad (14)$$

where, k is the conductivity of solution; d is the nominated diameter of the channel; ρ is the feed density; u is the feed velocity; μ is the feed viscosity; c_p is the specific heat at constant pressure of the feed.

The coefficient of condensation heat transfer could be described as follows:

$$h_{con} = 0.943 \left(\frac{\lambda_l^3 \cdot \rho_l^2 \cdot \lambda \cdot g}{l \cdot \mu_l \cdot \Delta T_{con}} \right)^{0.25} \quad (15)$$

where, λ_l is the heat condensate conductivity; ρ_l is the condensate density; λ is the latent heat of vapor; g is the acceleration of gravity; l is the length of wall; μ_l is the viscosity of condensate; ΔT_{con} is the temperature difference between condensate and plate.

The amount of convective heat transfer could be described as follows:

$$Q_c = M_6 H_6 + M_5 C_{p5} T_5 - M_4 C_{p4} T_4 \quad (16)$$

The amount of condensation heat transfer could be described as follows:

$$Q_{con} = M_7 H_7 - M_8 C_{p8} T_8 \quad (17)$$

In order to calculate conservatively, it was assumed that the heat transfer rate between condensation room and distillation room was the maximum from 363 K water vapor to 353 K condensate.

The amount of convective heat transfer should be equal to that of condensation heat transfer, described as follows:

$$M_6 H_6 + M_5 C_{p5} T_5 - M_4 C_{p4} T_4 = M_7 H_7 - M_8 C_{p8} T_8 \quad (18)$$

4.4 Thermodynamics of the compressor

The temperature of the permeate vapor could be increased after being compressed. The energy of the permeate vapor obtained could be related to the enthalpy change between the permeate vapor and the compressed vapor, which could be described as follows:

$$P = M_6 (H_7 - H_6) \quad (19)$$

where, P is the required power of compressor.

The heat permeate vapor obtained should be equal to the power output of the vapor compressor. Gas compressor thermodynamics would be the suitable theory to describe the process of vapor compression and transportation. The energy required for vapor compression and the relationship between temperature and pressure could be described respectively as follows (Ahmadi *et al.* 2017):

$$w = \frac{\psi}{\psi - 1} \frac{p_6 V_6}{\eta} \left(\varepsilon^{\frac{\psi-1}{\psi}} - 1 \right) \quad (20)$$

$$\frac{T_7}{T_6} = \left(\frac{p_7}{p_6} \right)^{\frac{\psi-1}{\psi}} \quad (21)$$

where, p_6 , p_7 are the pressure at the inlet and outlet of compressor, respectively; T_6 , T_7 are the temperature at the inlet and outlet of compressor, respectively; V_6 is volume

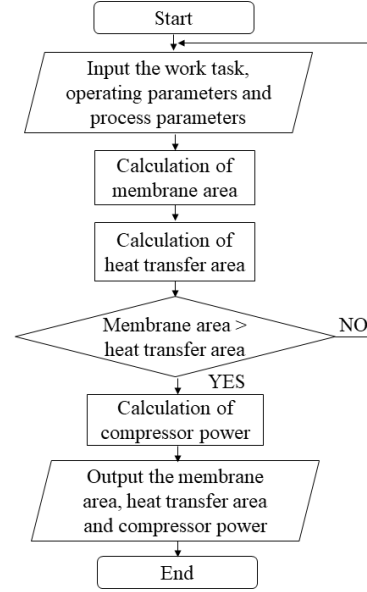


Fig. 4 Schematic diagram of numerical simulation

flowrate of vapor, ε is the compression ratio; ψ is the adiabatic exponent of the compression process; η is the adiabatic efficiency of the vapor compressor.

It should be noticed that, in order to simplify the formulas and calculations, it was assumed that the other working efficiency of compressor, including mechanical efficiencies, was taken as one in this system.

5. Results and discussion

5.1 The overall performance of the system

On the basis of the experiment of MD, the designed parameters used for the calculation of the mathematical models were illustrated in Table 2. The membrane area and power required by the vapor compressor were the two key issues of the hybrid desalination system combined MD and MVR, since the economic feasibility of the hybrid system were affected by the two issues. The calculated results including the membrane area and power required by the vapor compressor of the designed hybrid desalination process combined MD and MVR were illustrated in Table 3. It could be seen that only 75.24 m² of the membrane and 3.31 kW of electrical power were required to achieve 1000 kg h⁻¹ water treatment. It could be also seen that the required maximum heat transfer area was just about 66.72 m². The required membrane area being larger than the required heat transfer area meant that the heat transfer area was able to provide sufficient heat to evaporate the feed, since the heat transfer area was designed the same as the membrane area, as shown in Fig. 3. Moreover, 875 kg h⁻¹ water could be obtained during the operation of the hybrid desalination process, since the salinity in the concentrated solution was eight times higher than that in initial feed. It should be known that the membrane area, the required heat transfer area and power required by the vapor compressor could be affected by several designed and operation parameters.

Table 2 The designed parameters for the hybrid desalination system combined MD and MVR

Parameters	Value
Feed flow rate, kg h ⁻¹	1000
System Feed temperature, K	298
Feed mass concentration, %	1
Mass concentration in condensate, %	8
Temperature of condensate, K	308
Coefficient of convective heat transfer, W m ⁻² K ⁻¹	1763
Coefficient of condensation heat transfer, W m ⁻² K ⁻¹	1630
Conductivity of plate, W m ⁻² K ⁻¹	200
Total coefficient of heat transfer, W m ⁻² K ⁻¹	847
Mass transfer coefficient, s m ⁻¹	1.13
Adiabatic exponent	1.3
Efficiency of compressor	0.8

Table 3 The calculated results for the hybrid desalination system combined MD and MVR

Parameters	Value
Temperature difference of heat transfer, K	10
Pressure at the inlet of the compressor, kPa	26
Pressure at the outlet of the compressor, kPa	29
Feed temperature in membrane module, K	353
Required area of heat transfer, m ²	66.72
Required area of membrane, m ²	75.24
Compression ratio	1.13
Required power of compressor, kW	3.31

5.2 Effect of heat transfer temperature difference

Increasing or decreasing the temperature of the compressed vapor would change the heat transfer temperature difference, if the feed temperature in the membrane module was kept as a constant. The effect of heat transfer temperature difference between the feed and the compressed vapor in the membrane module on performance of the system was illustrated in Fig. 5. It could be seen that the required membrane area would not vary with the changing of the temperature difference due to the membrane flux was only depended on the vapor pressure between the two sides of the membrane. The required heat transfer area was decreased with the increasing heat transfer temperature difference. However, the decrease extent would be weakened gradually. It could be calculated that the required heat transfer area would decrease 60.0% if the heat transfer temperature difference was increased from 4 K to 10 K. This value was just 37.5%, if the heat transfer temperature difference was increased from 10 K to 16 K. Therefore, excessive increasing the heat transfer temperature difference to decrease the required heat transfer area would not be reasonable, since higher power of the

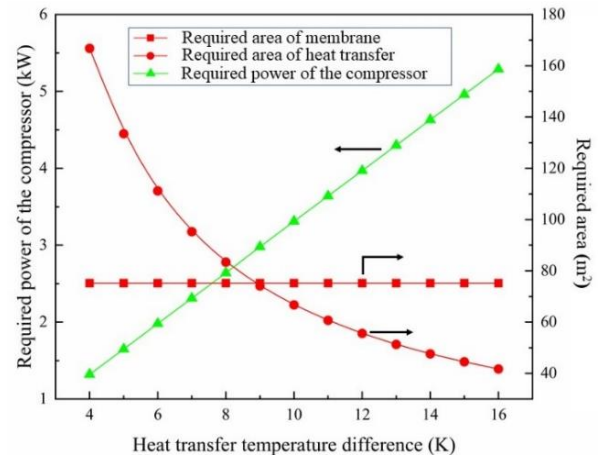


Fig. 5 The effect of the heat transfer temperature difference on performance of the hybrid desalination system combined MD and MVR

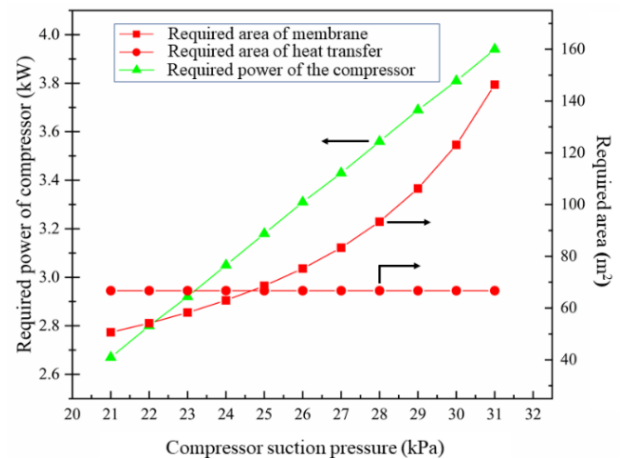


Fig. 6 The effect of the permeate vapor pressure on performance of the hybrid desalination system combined MD and MVR

vapor compressor must be required, as shown in Fig. 5.

From Fig. 3, it could be seen that the required heat transfer area and membrane area were assembled in a membrane module unit and the areas of the two parameters were designed as the same value. In order to provide sufficient heat for feed evaporation during MD process, the required heat transfer area should be less than that the designed value. In other words, the hybrid desalination system must be operated in a reasonable range, in which the required heat transfer area should be less than the required area of the membrane. Therefore, the heat transfer temperature difference should be higher than 9 K, as shown in Fig. 5.

5.3 Effect of compressor suction pressure

The compressor suction pressure was related to the heat and mass transfer during MD and the power of the vapor compressor. The effect on the hybrid desalination system was illustrated in Fig. 6. It could be seen that the required membrane area was increased with increasing compressor suction pressure. According to Eq. (7), it could be deduced

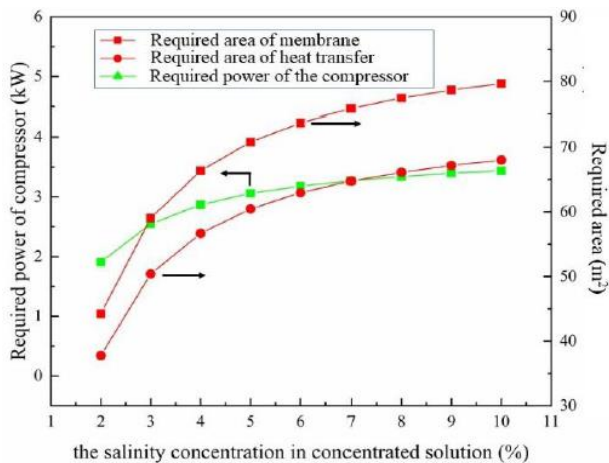


Fig. 7 The effect of salinity concentration in concentrated solution on performance of the hybrid desalination system combined MD and MVR

that higher compressor suction pressure would lead to lower mass transfer driving force and larger membrane area would be required to keep the constant capacity of the desalination system. It could be calculated that the required membrane area was increased 48.5% if the compressor suction pressure was increased from 21 kPa to 26 kPa. This value could be increased to be 94.5%, if the permeate vapor pressure was increased from 26 kPa to 31 kPa. In order to provide the sufficient heat for feed evaporation, the permeate vapor pressure should be higher than 25 kPa, as shown in Fig. 6.

Higher power would be required with increasing compressor suction pressure as indicated by Eq. (20). Therefore, the required power of the compressor was increased with the compressor suction pressure as shown in Fig. 6. Combined the required membrane area with required power of the vapor compressor, compressor suction pressure should be designed as 26 kPa.

5.4 Effect of the salinity concentration in concentrated solution

The concentration in concentrated solution was related to the fresh water amount produced in the hybrid system. In other words, the amount permeate vapor was dependent on the concentrated solution. The amount of the permeate vapor would be produced with the increase of the concentration in concentrated solution. Moreover, the mass transfer driving force would be decreased with increase of the concentration in concentrated solution, since the saturation pressure of the feed would be reduced. Therefore, both the required membrane area and power of the vapor compressor were increased with the increase of the concentration in concentrated solution, as shown in Fig. 7. Furthermore, the required area of heat transfer was also increased with the increase of the concentration in concentrated solution, since more water needed to be evaporated. It could be calculated that the required membrane area, heat transfer area and required power were increased 80.00%, 80.02% and 80.01%, respectively, with

the concentration in concentrated solution increased from 2 wt%-10 wt%.

6. Conclusions

The high desalination capacity of PTFE membrane was demonstrated by MD experiments. A desalination system combined MD and MVR with a capacity of 1000 kg h⁻¹ had been developed based on MD experiments. The developed mathematical models based on the energy conservation and mass conservation could be able to describe the system. 75.24 m² of the membrane and 3.31 kW of electrical power were required with 875 kg h⁻¹ fresh water obtained, under the condition of 10 K of heat transfer temperature difference, 353 K of feed temperature in membrane module and 26 kPa of compressor suction pressure. The system performances were greatly affected by some parameters when other parameters were kept constant. The variation of heat transfer temperature difference would cause a trade-off between compressor power and heat transfer area. Required compressor power, heat transfer area and membrane area would be higher when the salt concentration in the residual concentrate was higher.

The achievements of the study demonstrated the promising potential of the hybrid desalination system combined the high desalination rate of MD with the low energy consumption MVR. The future research would be conducted in the following aspects: (1) The membrane module of this structure should be fabricated and the simulated results should be verified with experimental results; (2) although PTFE membrane had inherent performance to resist biomacromolecule adhesion, the membrane fouling on MD needed to be investigated in order to achieve effective, stable and long-term process operation; (3) a comprehensive economic evaluation of the system should be conducted to verify its economic feasibility.

Acknowledgments

The present work is supported by the Fundamental Research Funds for the Central Universities (No.20822041B4013) and Key Laboratory of Development and Application of Rural Renewable Energy, Ministry of Agriculture, China (No. 18H0491).

References

- Ahmadi, M., Baniasadi, E. and Ahmadikia, H. (2017), "Process modeling and performance analysis of a productive water recovery system", *Appl. Therm. Eng.*, **112**, 100-110. <https://doi.org/10.1016/j.applthermaleng.2016.10.067>.
- Ahmed, F.E., Lalia, B.S., Hashaikeh, R. and Hilal, N. (2020), "Alternative heating techniques in membrane distillation: A review", *Desalination*, **496**, 114713. <https://doi.org/10.1016/j.desal.2020.114713>.
- Alasfour, F.N. and Abdulrahim, H.K. (2011), "The effect of stage temperature drop on MVC thermal performance", *Desalination*, **265**(1-3), 213-221. <https://doi.org/10.1016/j.desal.2010.07.054>.

- Boutikos, P., Mohamed, E.S., Mathioulakis, E. and Belessiotis, V. (2017), "A theoretical approach of a vacuum multi-effect membrane distillation system", *Desalination*, **422**, 25-41. <https://doi.org/10.1016/j.desal.2017.08.007>.
- Chang, H.Q., Liu, B., Wang, H., Zhang, S.Y., Chen, S., Tiraferri, A. and Tang, Y.Q. (2019), "Evaluating the performance of gravity-driven membrane filtration as desalination pretreatment of shale gas flowback and produced water", *J. Membrane Sci.*, **587**, 117187. <https://doi.org/10.1016/j.memsci.2019.117187>.
- Dahmardeh, H., Amiri, H.A. and Nowee, S.M. (2019), "Evaluation of mechanical vapor recompression crystallization process for treatment of high salinity wastewater", *Chem. Eng. Process. Intensif.*, **145**, 1097682. <https://doi.org/10.1016/j.cep.2019.107682>.
- El-Ghizizel, S., Jalte, H., Zeggar, H., Zait, M., Belhamidi, S., Tiyal, F., Hafsi, M., Taky, M. and Elmidaoui, A. (2019), "Autopsy of Nanofiltration membrane of a decentralized demineralization plant", *Membr. Water Treat.*, **10**(4), 277-286. <http://doi.org/10.12989/mwt.2019.10.4.277>.
- Gao, J.Y., Wang, M. and Yun, Y. (2018), "Treatment of high-salinity wastewater after the resin regeneration using VMD", *Membr. Water Treat.*, **9**(1), 53-62. <http://doi.org/10.12989/mwt.2018.9.1.053>.
- He, W.F., Zhu, W.P., Xia, J.R. and Han, D. (2018), "A mechanical vapor compression desalination system coupled with a transcritical carbon dioxide Rankine cycle", *Desalination*, **425**, 1-11. <https://doi.org/10.1016/j.desal.2017.10.009>.
- Hilal, N., Kochkodan, V., Al Abdulgader, H. and Johnson, D. (2015), "A combined ion exchange-nanofiltration process for water desalination: II. Membrane selection", *Desalination*, **363**, 51-57. <https://doi.org/10.1016/j.desal.2014.11.017>.
- Ihsanullah, I., Atieh, M.A., Sajid, M. and Nazal, M.K. (2021), "Desalination and environment: A critical analysis of impacts, mitigation strategies, and greener desalination technologies", *Sci. Total. Environ.*, **780**, 146585. <https://doi.org/10.1016/j.scitotenv.2021.146585>.
- Jamil, M.A. and Zubair, S.M. (2017), "On thermoeconomic analysis of a single-effect mechanical vapor compression desalination system", *Desalination*, **420**, 292-307. <https://doi.org/10.1016/j.desal.2017.07.024>.
- Karameldin, A., Lotfy, A. and Mekhemar, S. (2003), "The Red Sea area wind-driven mechanical vapor compression desalination system", *Desalination*, **153**(1-3), 47-53. [https://doi.org/10.1016/S0011-9164\(02\)01092-5](https://doi.org/10.1016/S0011-9164(02)01092-5).
- Kariman, H., Hoseinzadeh, S. and Hejns, P.S. (2019), "Energetic and exergetic analysis of evaporation desalination system integrated with mechanical vapor recompression circulation", *Case Stud. Therm. Eng.*, **16**, 100548. <https://doi.org/10.1016/j.csite.2019.100548>.
- Kim, Y.D., Kim, Y.B. and Woo, S.Y. (2018), "Detailed modeling and simulation of an out-in configuration vacuum membrane distillation process", *Water Res.*, **132**, 23-33. <https://doi.org/10.1016/j.watres.2017.12.066>.
- Liang, L., Han, D., Ma, R. and Peng, T. (2013), "Treatment of high-concentration wastewater using double-effect mechanical vapor recompression", *Desalination*, **314**, 139-146. <https://doi.org/10.1016/j.desal.2013.01.016>.
- Liang, L., Li, Y. and Talpur, M.A. (2017), "Analysis of a double-effect mechanical vapor recompression wastewater treatment system", *Desalin. Water Treat.*, **66**, 1-9. <https://doi.org/10.5004/dwt.2016.0152>.
- Luo, A.Y. and N. Lior (2017), "Study of advancement to higher temperature membrane distillation", *Desalination*, **419**, 88-100. <https://doi.org/10.1016/j.desal.2017.05.020>.
- Luo, W.H., Phan, H.V., Li, G., Hai, F.I., Price, W.E., Elimelech, M. and Nghiem, L.D. (2017), "An osmotic membrane bioreactor-membrane distillation system for simultaneous wastewater reuse and seawater desalination: Performance and implications", *Environ. Sci. Technol.*, **51**(24), 14311-14320. <https://doi.org/10.1021/acs.est.7b02567>.
- Lv, H., Wang, Y., Wu, L. and Hu, Y. (2019), "Numerical simulation and optimization of the flash chamber for multi-stage flash seawater desalination", *Desalination*, **465**, 69-78. <https://doi.org/10.1016/j.desal.2019.04.032>.
- Onishi, V.C., Carrero-Parreño, A., Reyes-Labarta, J.A., Ruiz-Femenia, R., Salcedo-Díaz, R., Fraga, E.S. and Caballero, J.A. (2017), "Shale gas flowback water desalination: Single vs multiple-effect evaporation with vapor recompression cycle and thermal integration", *Desalination*, **404**, 230-248. <https://doi.org/10.1016/j.desal.2016.11.003>.
- Si, Z.T., Han, D., Gu, J., Song, Y. and Liu, Y. (2020), "Exergy analysis of a vacuum membrane distillation system integrated with mechanical vapor recompression for sulfuric acid waste treatment", *Appl. Therm. Eng.*, **178**, 115516. <https://doi.org/10.1016/j.applthermaleng.2020.115516>.
- Si, Z.T., Han, D., Song, Y., Chen, J., Luo, L. and Li, R. (2019), "Experimental investigation on a combined system of vacuum membrane distillation and mechanical vapor recompression", *Chem. Eng. Process. Intensif.*, **139**, 172-182. <https://doi.org/10.1016/j.cep.2019.04.007>.
- Wang, J., Zheng, L., Wu, Z., Zhang, Y. and Zhang, X. (2016), "Fabrication of hydrophobic flat sheet and hollow fiber membranes from PVDF and PVDF-CTFE for membrane distillation", *J. Membrane Sci.*, **497**, 183-193. <https://doi.org/10.1016/j.memsci.2015.09.024>.
- Yang, J., Zhang, C., Zhang, Z., Yang, L. and Lin, W. (2016), "Study on mechanical vapor recompression system with wet compression single screw compressor", *Appl. Therm. Eng.*, **103**, 205-211. <https://doi.org/10.1016/j.applthermaleng.2016.04.053>.
- Zhou, S.H., Gong, L., Liu, X. and Shen, S. (2019), "Mathematical modeling and performance analysis for multi-effect evaporation/multi-effect evaporation with thermal vapor compression desalination system", *Appl. Therm. Eng.*, **159**, 113759. <https://doi.org/10.1016/j.applthermaleng.2019.113759>.

CC

Nomenclature

A	heat transfer area, m^2
A_m	membrane area, m^2
CF	correction coefficient for plate combination
C_p	specific heat at constant pressure, $kJ\ kg^{-1}\ K^{-1}$
d	nominated diameter of the channel, m
F	flux of membrane, $kg\ m^{-2}\ h^{-1}$
g	acceleration of gravity, $m\ s^{-2}$
h	coefficient of heat transfer, $W\ m^{-2}\ K^{-1}$

H	specific enthalpy, kJ kg^{-1}	λ	latent heat of vapor, kJ kg^{-1}
k	heat conductivity coefficient, $\text{W m}^{-2} \text{K}^{-1}$	μ	viscosity, Pa s
K_m	number of distillation efficiency, s m^{-1}	η	adiabatic efficiency
l	length of wall, m	ε	compression ratio
M	mass flow rate, kg s^{-1}	γ	activity coefficient
P	the required power of vapor compressor, kW	ψ	adiabatic exponent
P_i	ideal power required by vapor compressor, kW	Subscripts	
ΔP	pressure difference on both sides of membrane, kPa	c	convective
P_p	vacuum pressure, kPa	con	condensation
Q	heat flow rate, J s^{-1}	fm	membrane surface
r	fouling resistance of heat transfer, $\text{m}^2 \text{kW}^{-1}$	l	liquid
R	gas constant, $\text{kJ kg}^{-1} \text{K}^{-1}$	m	membrane
T	temperature, K	i	ideal
ΔT	temperature difference, K	s	solution
u	feed velocity, m s^{-1}	v	vapor
U	total coefficient of heat transfer, $\text{W m}^{-2} \text{K}^{-1}$	w	water
w	specific power of compressor, kJ kg^{-1}	$1 \rightarrow 12$	fluid
x	molar fraction		
X	mass concentration, %		

Greek letters

δ	heat conduction thickness, m
ρ	density of liquid, kg m^{-3}